Microscopic theory of spin arrangements and spin waves in very thin ferromagnetic films

R. P. Erickson and D. L. Mills

Department of Physics, University of California, Irvine, Irvine, California 92717

(Received 9 October 1990)

We present theoretical studies of the classical ground-state spin configuration and spin waves, in very thin ferromagnetic films, with thickness that ranges from a monolayer to a few tens of layers. The analyses are based on a microscopic model that includes dipolar and exchange interactions between the spins, surface (or interface) anisotropy of single-site character quadratic and quartic in the spin components, along with an external magnetic field applied at an arbitrary direction with respect to the film normal. Issues explored include the nature of spin canting induced by surface anisotropy in ultrathin (few-atomic-layer) films, and in films with thicknesses of up to 100 layers. Also, we explore the nature of spin waves in ultrathin films, in the presence of spin canting, and in thicker films with attention to the interplay between dipolar and exchange contributions to the excitation energy. Most particularly, in the thicker films, we examine the transition from the dipole-dominated Damon-Eshbach waves to the exchange-dominated surface spin waves that emerge from the Heisenberg model.

I. INTRODUCTION

There is currently great interest in the properties of very thin ferromagnetic films, with thicknesses in the range of a few atomic layers. The ferromagnetic properties of such films can differ dramatically from those of bulk crystals of the same material. For example, ultrathin films of Fe can exhibit strong uniaxial anisotropies,[1] characterized by anisotropy energies larger than those realized in bulk Fe by roughly two orders of magnitude. This is, one presumes, a consequence of the low site symmetry at the surfaces and interfaces of a few-atomic-layer film, while in bulk Fe all atoms reside at sites of cubic symmetry.[2] The uniaxial anisotropy can render the axis normal to the film an easy axis. When the film thickness in this case is sufficiently thin, the uniaxial anisotropy can overwhelm the dipolar energies, which favor alignment of the magnetization parallel to the film surfaces. A consequence is that the magnetization of the film will orient normal rather than parallel to the surfaces. In a recent experiment, the spins in a few-atomic-layer film have been found to reorient, with respect to the film surfaces, from normal to parallel, as temperature increases.[3] In such thin films, the spins can also be found canted from the film normal.

One can also carry out experimental studies of (long-wavelength) spin waves in few-atomic-layer films. Two techniques have been successfully used in such experiments. One is ferromagnetic resonance,[4] and the second is light scattering (Brillouin scattering).[5,6] Both methods can explore the surface magnetic response of thick crystals,[7] multilayers or superlattices possibly fabricated from few-atomic-layer films, and isolated ultrathin films only a few layers in thickness.[6]

These data are generally analyzed by applying theoretical descriptions developed for films or samples whose thickness or linear dimensions are macroscopic; such theories are then applied to few-atomic-layer films. While many features of the data on ultrathin films are accounted for nicely by such a procedure,[6] it is clearly desirable to utilize a fully macroscopic description of the film.

There are in fact questions which are difficult to answer within the macroscopic theory. For example, light scattering studies of ultrathin Fe films have explored the low-frequency spin-wave branch of a few-monolayer Fe film.[6] As noted earlier, a macroscopic description of this wave, in the limit $k_\parallel = 0$, where $k_\parallel$ is its wave vector parallel to the film surfaces, accounts for the data very well. Such a theory, in our view, would provide a questionable description of the dispersion relation of this branch. The film studied in Ref. 6 is three atomic layers thick; two-thirds of the spins reside in either a surface or in the interface between the film and the substrate. Thus introduction of the influence of exchange by adding the $-D\nabla^2$ term to the equations of motion of the appropriate spin components would be inappropriate. If one wished to examine the temperature dependence of the magnetization of the film through the use of spin-wave theory,[8] the dispersion relation of this low-frequency branch would play a key role.

There is another issue of interest to us that has yet to be addressed, and which cannot be addressed within a macroscopic theory. At long wave-lengths, spin-wave excitation energies are dominated by the Zeeman and dipolar contributions (and in thin films, surface or interface anisotropy enters as well). Exchange, however, plays a minor role. In this regime, one encounters a surface spin wave known as the Damon-Eshbach wave. The frequency of this wave lies *above* those of the very-long-wavelength bulk spin waves.[9] At shorter wavelengths, spin-wave excitation energies are dominated by exchange couplings between the spins, while Zeeman and dipolar contributions are small. Numerous theoretical studies of

the semi-infinite Heisenberg ferromagnet of exchange coupled spins shows that one encounters surface spin waves whose frequency lies *below* the bulk spin-wave frequencies. For exchange surface spin waves whose wavelength is long compared to a lattice constant, the difference in frequency between the surface wave and the lowest-frequency bulk wave scales as $k_{\parallel}^4$ for a wide variety of surface geometries.

It follows that one can never describe such exchange-dominated surface spin waves by any theory that introduces the influence of exchange only through the use of a term of the form $-D\nabla^2$ in the equations of motion; one must have terms fourth order in the various spatial derivatives. The transition between the dipole-dominated Damon-Eshbach regime and the exchange-dominated regime described by the Heisenberg model thus has not been addressed in the literature. Introduction of the $-D\nabla^2$ term in the equation of motion, in combination with the appropriate boundary conditions at the surfaces or interfaces, gives an adequate description of the effects of exchange at long wavelengths,[10,11] but one never achieves a proper account of the exchange-dominated region.

In this paper, we present a study of spin arrangements and spin waves in thin ferromagnetic films by means of a fully microscopic model. We begin with a film of an assumed microscopic structure, chosen to be either fcc or bcc in character with (100) surfaces for results presented here. We employ a microscopic description of the dipolar interactions and exchange couplings, along with anisotropy in the surfaces or interfaces. There is also a spatially uniform magnetic field, applied in an arbitrary direction. We begin by finding the (classical) ground state by means of an energy-minimization procedure. In the presence of surface anisotropy, the spins may be canted, with a layer-dependent canting angle. Once the classical ground state is determined, we then study the spin-wave excitations of the canted array. In this work, we address issues such as those mentioned above, which are difficult to address within the macroscopic approach. We can also compare our results with the macroscopic description of the model system, and thus delineate the range of validity of this approach.

In the course of the analysis, one encounters certain spatial Fourier transforms of dipole sums. The dipole sums are long ranged, and the resulting expressions thus converge very slowly. However, through methods discussed some years ago,[12] it is possible to convert these dipole sums to series that converge very rapidly.

Our model is limited in some regards, of course. We have a lattice of localized spins coupled as described above, and ultimately we have applications to ultrathin films of Fe in mind; Fe is of course an itinerant ferromagnet, and one questions the applicability of the Heisenberg model to such a material. We regard our approach as phenomenological because of this. In our numerical work, we adjust the strength of the nearest-neighbor exchange so the value of the spin-wave exchange stiffness D is reproduced properly. We then obtain a proper description of the response of Fe to long-wavelength disturbances in the spin system, while the results for excitations

that involve the short-wavelength response must be viewed as an extrapolation. Also, at the time of this writing, we have virtually no data in hand that provides reliable information on the nature of the effective exchange couplings within the ultrathin films, and in their surfaces and interfaces.

II. FORMULATION OF THE THEORY

A. The microscopic model

Our model for a thin ferromagnetic film consists of N layers, stacked to form a cubic crystal, with one atom per unit cell, in the bulk realization of the structure. We have two (100) surfaces that are planar, and infinite in extent. The calculations reported here are for films of fcc and bcc structure. The Hamiltonian includes nearest-neighbor Heisenberg exchange, dipole-dipole coupling between spins on the lattice, and surface anisotropy that introduces an easy axis normal to the film surfaces. The surface anisotropy includes contributions from terms quadratic and quartic in the relevant spin components. We also allow for the application of a spatially uniform magnetic field $\mathbf{H}_{ex}$ of arbitrary magnitude and orientation.

The Hamiltonian for this model may then be expressed in the form

$$H = -\frac{1}{2S}\left[\sum_{l,l'}\mathbf{S}(l)\cdot\mathbf{A}(l,l')\cdot\mathbf{S}(l')\right.$$
$$\left.+\sum_l\left[h_{s_1}(l_\perp)S_\perp^2(l)+\frac{1}{2S^2}h_{3_2}(l_\perp)S_\perp^4(l)\right]\right]$$
$$-\sum_l\mathbf{H}_{ex}\cdot\mathbf{S}(l) \tag{1a}$$

where $\mathbf{S}(l)$ is the operator associated with the spin of length S corresponding to the site l. The subscript $\perp$ denotes components of a vector normal to the film surfaces. For a cubic film, corresponding to a material with bulk lattice constant a_0 and unit-cell volume V_0, we may write the real, symmetric exchange and dipole tensor $\mathbf{A}(l,l')$ in the form, for $l\neq l'$,

$$\Lambda_{\alpha\beta}(l,l') = \frac{D}{a_0^2}\sum_\delta \delta_{l,l'+\delta}\delta_{\alpha\beta} - M_s d_{\alpha\beta}(l,l') . \tag{1b}$$

Here, D is the spin-wave exchange stiffness constant, expressed in units of G cm^2, M_s is the saturation magnetization, the sum on δ ranges over the sites that are nearest neighbors to l, and

$$d_{\alpha\beta}(l,l') = V_0\frac{\delta_{\alpha\beta}-3\hat{x}_\alpha(l,l')\hat{x}_\beta(l,l')}{|\mathbf{x}(l,l')|^3} \tag{1c}$$

with $\mathbf{x}(l,l')$ a vector directed from site l to site l', and $\hat{x}(l,l')$ its corresponding unit vector. One has $\Lambda_{\alpha\beta}(l,l)\equiv 0$. We can easily allow for changes in exchange constants in and near the film surfaces, but since very little unambiguous information is available on this

question at this time, we set the exchange constants equal to their bulk values everywhere.

Also, $h_{s_1}(l_\perp)$ and $h_{s_2}(l_\perp)$ are measures of the strength of the uniaxial anisotropy quadratic and quartic in the spin components, respectively. In the calculations discussed here, we assume the surface anisotropy to be the same on each surface. Thus we write

$$h_{s_i}(l_\perp) = h_{s_i}(\delta_{1l_\perp} + \delta_{Nl_\perp}), \quad i = 1, 2 , \tag{1d}$$

where h_{s_i} is a constant, measured in magnetic-field units. It is possible, of course, for there to be uniaxial anisotropy on interior layers of the film, particularly in the ultrathin films. Very little is known about this question at the time of this writing, so we adopt this simple picture as a model.

From the Hamiltonian given above, we may calculate the equation of motion of the spin $\mathbf{S}(l)$. When this is done, and the operators are treated classically [by replacing $S_x(l)S_z(l) + S_z(l)S_x(l)$ by $2S_z(l)S_x(l)$, for instance], one finds

$$\frac{\partial}{\partial t}\mathbf{S}(l,t) = \mathbf{S}(l,t) \times \mathbf{H}(l,t) , \tag{2a}$$

where $\mathbf{H}(l,t)$ is an effective magnetic field at lattice site l, defined as

$$\mathbf{H}(l,t) = \mathbf{H}_{ex} + \frac{1}{S}\sum_{l'}\mathbf{\Lambda}(l,l')\cdot\mathbf{S}(l',t)$$
$$+ \frac{1}{S}\left[h_{s_1}(l_\perp) + \frac{1}{S^2}h_{s_2}(l_\perp)S_1^2(l,t)\right]\mathbf{S}_\perp(l,t) . \tag{2b}$$

These equations of motion allow us to explore both the nature of the classical ground state and the spin-wave spectrum of the film.

B. Determination of the classical ground state

We first begin by finding the static ground-state spin arrangement. We establish a laboratory coordinate system, and we allow for the possibility that the spins may be canted in a layer by layer fashion. Thus we construct a local coordinate system in each layer, with its z axis aligned along the direction of the spins in that layer. We then seek the transformation between the laboratory coordinate system, and the local coordinate system associated with the various layers. We then linearize the equations of motion about the equilibrium arrangement, to generate spin waves. Since the film possesses translational symmetry parallel to the surfaces, it is reasonable
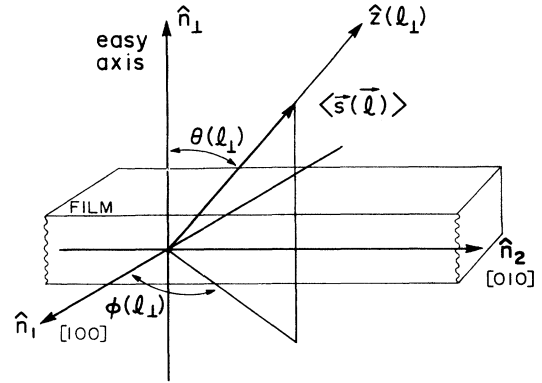
FIG. 1. The local z axis of quantization, $\hat{z}(l_\perp)$, for the film layer $l_\perp$, which defines the spin orientation for this layer, in the classical ground state.

to suppose each spin in a given layer has the same orientation in the ground state. The transformations are then a function of the angles that describe the rotation from the laboratory system to that associated with the various layers.

Let $\hat{z}(l_\perp)$ describe the z direction corresponding to layer $l_\perp$; the spins in this layer are thus parallel to $\hat{z}(l_\perp)$. As indicated in Fig. 1, $\theta(l_\perp)$ and $\phi(l_\perp)$ are the spherical polar coordinates that define the orientation of $\hat{z}(l_\perp)$ with respect to the film normal. The rotation from the laboratory frame to the local frame corresponding to layer $l_\perp$ can then be written $\underline{R}_z(\phi(l_\perp))\underline{R}_y(\theta(l_\perp))$, where $\underline{R}_\beta(\alpha)$ is a rotation by the angle α about the β axis, in the convention of active Euler rotations.[13] In addition, we include a transformation to the spin raising and lowering operators $S_\pm(l,t)$ rather than the Cartesian components $S_{x,y}(l,t)$. This is generated by the unitary matrix $\underline{U}$,

$$\underline{U} = \begin{bmatrix} \dfrac{1}{\sqrt{2}} & \dfrac{1}{\sqrt{2}} & 0 \\[2mm] -\dfrac{i}{\sqrt{2}} & \dfrac{i}{\sqrt{2}} & 0 \\[2mm] 0 & 0 & 1 \end{bmatrix} . \tag{3}$$

Hence the complete transformation between the laboratory frame and the frame associated with a given layer is $\underline{T}(\theta(l_\perp),\phi(l_\perp)) = \underline{R}_z(\phi(l_\perp))\underline{R}_y(\theta(l_\perp))\underline{U}$. We shall refer to this operator as $\underline{T}(l_\perp)$ in what follows. One has the explicit form, omitting reference to the layer index $l_\perp$,

$$\underline{T} = \begin{bmatrix} \dfrac{1}{\sqrt{2}}(\cos\phi\cos\theta + i\sin\phi) & \dfrac{1}{\sqrt{2}}(\cos\phi\cos\theta - i\sin\phi) & \cos\phi\sin\theta \\[3mm] \dfrac{1}{\sqrt{2}}(\sin\phi\cos\theta - i\cos\phi) & \dfrac{1}{\sqrt{2}}(\sin\phi\cos\theta + i\cos\phi) & \sin\phi\sin\theta \\[3mm] -\dfrac{1}{\sqrt{2}}\sin\theta & -\dfrac{1}{\sqrt{2}}\sin\theta & \cos\theta \end{bmatrix} . \tag{4}$$

Given a vector, such as the spin $\mathbf{S}(l,t)$ with laboratory components $(S_1(l,t), S_2(l,t), S_\perp(l,t))$, the relation to the spin components of $\mathbf{s}(l,t)$ in the local film plane is

$$\mathbf{S}(\mathbf{l},t) = \underline{T}(l_\perp) \cdot \mathbf{s}(l,t) . \tag{5}$$

The vector $\mathbf{s}(l,t)$ has the components

$$\mathbf{s}(l,t) = \begin{vmatrix} \dfrac{1}{\sqrt{2}} S_+(l,t) \\[2mm] \dfrac{1}{\sqrt{2}} S_-(l,t) \\[2mm] S_z(l,t) \end{vmatrix} \tag{6}$$

expressed in the layer coordinate system illustrated in Fig. 1. A similar relation holds between the magnetic field $\mathbf{H}(l,t)$, and that of $\mathbf{h}(l,t)$ reckoned in the layer-dependent coordinate system.

Let $\langle \mathbf{S}(l_\perp) \rangle = S\hat{\mathbf{z}}(l_\perp)$ be the equilibrium spin direction in layer $l_\perp$, and $\langle \mathbf{H}(l_\perp) \rangle$ the static magnetic field which acts on the spins in layer $l_\perp$, when all spins are frozen in the ground-state spin configuration. For the system to be in equilibrium, we require

$$\langle \mathbf{S}(l_\perp) \rangle \times \langle \mathbf{H}(l_\perp) \rangle = S\hat{\mathbf{z}}(l_\perp) \times \langle \mathbf{H}(l_\perp) \rangle = 0 . \tag{7}$$

We should comment briefly on the regime of validity of this approximation scheme. When we utilize Eq. (7) to determine the classical ground state, and analyze the spin-wave spectra as we do below, we are ignoring the role of quantum spin fluctuations, a procedure that is exact in the limit $S \to \infty$. The procedure is used widely in magnetism, and is known to work well even for modest values of the spin S. For example, in the exchange coupled ferromagnet, quantum-mechanical fluctuations are rigorously absent in the ground state, and are present only if magnetic dipole interactions are incorporated into the theory. Their influence on the properties of the three-dimensional ferromagnet was explored in the original classic paper by Holstein and Primakoff,[14] and found to be very modest for parameters characteristic of materials of interest here. Spin canting induces quantum fluctuations also, but these are modest in three-dimensional crystals even for S as small as unity, as one can see from analyses of the classic two sublattice antiferromagnet.[15] The ultrathin films of interest here are in fact quasi-two-dimensional; this may raise concern about the use of the classical ground state. We note, however, that classical spin-wave theory, based on the classical ground state, provides a fully quantitative account of the quasi-two-dimensional antiferromagnet K_2NiF_4, where $S=1$. There are, however, substantial corrections from quantum fluctuations, ignored here, when $S = \frac{1}{2}$ for quasi-two-dimensional materials.[16]

Of course, the statement $\langle \mathbf{S}(l_\perp) \rangle = S\hat{\mathbf{z}}(l_\perp)$ also requires we be at sufficiently low temperature for the magnetization at each site to be well approximated by its value at $T=0$. A full treatment of the effect of finite temperatures on the spin-wave spectrum in the presence of surfaces is rather complex, unfortunately, as one can see from an earlier discussion of this question.[17]

We have, from Eq. (2b),

$$\langle \mathbf{H}(l_\perp) \rangle = \mathbf{H}_{ex} + \sum_{l'} \mathbf{\Lambda}(l,l') \cdot \hat{\mathbf{z}}(l'_\perp)$$
$$+ [h_{s_1}(l_\perp) + h_{s_2}(l_\perp)\cos^2\theta(l_\perp)]\cos\theta(l_\perp)\hat{\mathbf{n}}_\perp , \tag{8}$$

here $\hat{\mathbf{n}}_\perp$ is normal to the film surfaces (Fig. 1). From Fig. 1, it is easy to see that $\phi(l_\perp)$ and $\theta(l_\perp)$ are given by

$$\tan\phi(l_\perp) = \frac{\langle H_2(l_\perp) \rangle}{\langle H_1(l_\perp) \rangle} \tag{9a}$$

and

$$\tan\theta(l_\perp) = \frac{\langle H_\parallel(l_\perp) \rangle}{\langle H_\perp(l_\perp) \rangle} , \tag{9b}$$

where $\langle H_\parallel(l_\perp) \rangle$ and $\langle H_\perp(l_\perp) \rangle$ are the components of $\langle \mathbf{H}(l_\perp) \rangle$ parallel and perpendicular to the film surfaces.

As an explicit example, suppose the external field $\mathbf{H}_{ex}$ is parallel to the film surfaces, and to the [100] direction. This is the direction of $\hat{\mathbf{n}}_1$ in Fig. 1. The ground state will have all spins in the plane defined by the normal to the film and $\mathbf{H}_{ex}$. Thus all the angles $\phi(l_\perp)$ vanish. Then Eq. (9b) can be written

$$\tan\theta(l_\perp) = \frac{\langle H_1(l_\perp) \rangle}{\langle H_\perp(l_\perp) \rangle} , \quad 1 \le l_\perp \le N . \tag{10}$$

From Eqs. (1b), (1d), and (8), and through exploiting cubic symmetry, we have

$$\langle H_1(l_\perp) \rangle = H_{ex} + \sum_{l'_\perp} \left[\frac{D}{a_0^2} z(l_\perp, l'_\perp) - M_s d_{11}(l_\perp, l'_\perp) \right] \sin\theta(l'_\perp) \tag{11a}$$

and

$$\langle H_\perp(l_\perp) \rangle = \sum_{l'_\perp} \left[\frac{D}{a_0^2} z(l_\perp, l'_\perp) - M_s d_{\perp\perp}(l_\perp, l'_\perp) \right] \cos\theta(l'_\perp)$$
$$+ (\delta_{1,l_\perp} + \delta_{N,l_\perp})[h_{s_1} + h_{s_2}\cos^2\theta(l_\perp)]$$
$$\times \cos\theta(l_\perp) , \tag{11b}$$

where $z(l_\perp, l'_\perp)$ is the number of nearest neighbors of a site in layer $l_\perp$, which reside in layer $l'_\perp$. By $d_{\alpha\beta}(l_\perp, l'_\perp)$ we mean

$$d_{\alpha\beta}(l_\perp, l'_\perp) = \sum_{l'_\parallel} d_{\alpha\beta}(l,l') . \tag{12}$$

Sums such as this can be expressed as rapidly converging series, through techniques discussed some years ago.[12]

We had no difficulty finding minimum-energy configurations $\{\theta(l_\perp)\}$ that satisfied the above equations for a very wide range of film thicknesses, pinning field magnitudes h_{s_1} and h_{s_2}, and external field strengths H_{ex}. Our approach was to use a simple iteration procedure, that of rotating the spins of a given layer $l_\perp$ into the local field $\langle H(l_\perp) \rangle$, until self-consistency was achieved. One begins with a guess for the various $\theta(l_\perp)$, substituting them into Eqs. (11), then using Eq. (10) to generate a new

set of $\theta(l_\perp)$. When we found a canted spin arrangement, we compared its energy to the case where $\{\theta(l_\perp)=\pi/2\}$, that of all spins parallel to the film surfaces. We shall discuss the results of these calculations in Sec. III.

C. Small amplitude spin waves

The equations of motion that describe small amplitude spin waves, possibly excited from a canted ground state, can be obtained through further use of the transformation $\underline{T}(l_\perp)$ introduced above.

When a spin is excited, we may write

$$\mathbf{S}(l,t)=\langle \mathbf{S}(l_\perp)\rangle+\Delta\mathbf{S}(l,t) \tag{13a}$$

for the spin on site l, and for the magnetic field at site l, we have a similar decomposition:

$$\mathbf{H}(l,t)=\langle \mathbf{H}(l_\perp)\rangle+\Delta\mathbf{H}(l,t) . \tag{13b}$$

Since the transformation effected by $\underline{T}(l_\perp)$ is linear, we have

$$\Delta\mathbf{S}(l,t)=\underline{T}(l_\perp)\cdot\Delta\mathbf{s}(l,t) \tag{14a}$$

with

$$\Delta\mathbf{s}(l,t)=\begin{vmatrix}\dfrac{1}{\sqrt{2}}S_+(l,t)\\[2mm]\dfrac{1}{\sqrt{2}}S_-(l,t)\\[2mm]\Delta S_z(l,t)\end{vmatrix} , \tag{14b}$$

where as discussed earlier, the Cartesian components of the quantities in $\Delta\mathbf{s}(l,t)$ are determined in the coordinate system oriented with z axis aligned along the direction of the spins in layer $l_\perp$. Similarly, we have

$$\Delta\mathbf{H}(l,t)=\underline{T}(l_\perp)\cdot\Delta\mathbf{h}(l,t) , \tag{15a}$$

where

$$\Delta\mathbf{h}(l,t)=\begin{vmatrix}\dfrac{1}{\sqrt{2}}H_+(l,t)\\[2mm]\dfrac{1}{\sqrt{2}}H_-(l,t)\\[2mm]0\end{vmatrix} . \tag{15b}$$

We substitute these forms into the equations of motion, Eq. (2a), noting the spins are arranged so the equilibrium condition in Eq. (7) is satisfied. One then finds, noting

$\Delta S_z(l,t)$ may be set to zero since this is second order in the spin-wave amplitude,

$$\frac{\partial}{\partial t}\Delta\mathbf{S}(l,t)=\langle \mathbf{S}(l_\perp)\rangle\times\Delta\mathbf{H}(l,t)-\langle \mathbf{H}(l_\perp)\rangle\times\Delta\mathbf{S}(l,t)$$

$$\tag{16a}$$

or

$$i\frac{\partial}{\partial t}S_\pm(l,t)=\pm[\langle H(l_\perp)\rangle S_\pm(l,t)-SH_\pm(l,t)] . \tag{16b}$$

Here $\langle H(l_\perp)\rangle$ is the magnitude of the field seen by spins in layer $l_\perp$ in the ground state; this is parallel to the z axis in the coordinate system aligned with the canted spins.

Combining the various approximations above allows one to write

$$H_\pm(l,t)=\frac{1}{S}\sum_{l'}[\Delta^R(l,l')\cdot\Delta\mathbf{s}_\parallel(l',t)]_\pm$$

$$+\frac{1}{S}h_s(l_\perp)\sin^2\theta(l_\perp)[S_+(l,t)+S_-(l,t)] , \tag{17}$$

where

$$\underline{\Delta}^R(l,l')=\underline{T}^\dagger(l_\perp)\Lambda(l,l')\underline{T}(l'_\perp) , \tag{18a}$$

$$\Delta\mathbf{s}_\parallel(l,t)=\begin{vmatrix}S_+(l,t)\\S_-(l,t)\\0\end{vmatrix} , \tag{18b}$$

and

$$h_s(l_\perp)=\tfrac{1}{2}[h_{s_1}(l_\perp)+3h_{s_2}(l_\perp)\cos^2\theta(l_\perp)] . \tag{18c}$$

We seek solutions of the equations of motion of the form

$$S_\pm(l,t)=S_\pm(\mathbf{k}_\parallel,l_\perp)e^{i\mathbf{k}_\parallel\cdot\mathbf{x}(l)-i\Omega(\mathbf{k}_\parallel)t} . \tag{19}$$

The frequency $\Omega(\mathbf{k}_\parallel)$ of the spin wave is measured in magnetic-field units. We may substitute Eq. (19) into the equations of motion, to obtain, in a notation where the subscripts refer to $+$ and $-$, the basic eigenvalue equation

$$\sum_{l'_\perp=1}^{N}\sum_{\beta=\pm}\mathcal{D}_{\alpha\beta}(\mathbf{k}_\parallel;l_\perp,l'_\perp)S_\beta(\mathbf{k}_\parallel;l'_\perp)=S_\alpha(\mathbf{k}_\parallel;l_\perp) . \tag{20}$$

The 2×2 matrix $\underline{\mathcal{D}}(\mathbf{k}_\parallel;l_\perp,l'_\perp)$, whose components are $\mathcal{D}_{\alpha\beta}(\mathbf{k}_\parallel;l_\perp,l'_\perp)$, is given by

$$\underline{\mathcal{D}}(\mathbf{k}_\parallel;l_\perp,l'_\perp)=\begin{bmatrix}\langle H(l_\perp)\rangle-h_s(l_\perp)\sin^2\theta(l_\perp) & -h_s(l_\perp)\sin^2\theta(l_\perp)\\[2mm]h_s(l_\perp)\sin^2\theta(l_\perp) & -\langle H(l_\perp)\rangle+h_s(l_\perp)\sin^2\theta(l_\perp)\end{bmatrix}\delta_{l_\perp,l'_\perp}$$

$$+\begin{bmatrix}-\Lambda^R_{++}(\mathbf{k}_\parallel;l_\perp,l'_\perp) & -\Lambda^R_{+-}(\mathbf{k}_\parallel;l_\perp,l'_\perp)\\[2mm]\Lambda^R_{-+}(\mathbf{k}_\parallel;l_\perp,l'_\perp) & \Lambda^R_{--}(\mathbf{k}_\parallel;l_\perp,l'_\perp)\end{bmatrix} . \tag{21}$$

One has

$$\Lambda_{\alpha\beta}^R(\mathbf{k}_\parallel; l_\perp, l_\perp') = \sum_{l_\parallel'} \Lambda_{\alpha\beta}^R(\mathbf{l}, \mathbf{l}') e^{-i\mathbf{k}_\parallel \cdot \mathbf{x}(\mathbf{l}, \mathbf{l}')} . \tag{22}$$

In the above structures, we encounter the dipole sums

$$d_{\alpha\beta}(\mathbf{k}_\parallel; l_\perp, l_\perp') = V_0 \sum_{l_\parallel'} \frac{\delta_{\alpha\beta} - 3\hat{x}_\alpha(\mathbf{l}, \mathbf{l}')\hat{x}_\beta(\mathbf{l}, \mathbf{l}')}{|\mathbf{x}(\mathbf{l}, \mathbf{l}')|^3} e^{-i\mathbf{k}_\parallel \cdot \mathbf{x}(\mathbf{l}, \mathbf{l}')} . \tag{23}$$

As remarked earlier, these sums can be converted into rapidly converging forms, including the most slowly converging sums,[12] those for which $l_\perp = l_\perp'$. One can then evaluate the dipole sums to six-figure accuracy by including roughly 100 terms. An exception is some of the calculations of spin-wave spectra reported below where $k_\parallel a_0$ is very small compared to unity, say in the range of 0.01. Then as many as 100 000 terms are required to maintain six-digit accuracy. Hence we were able to solve for the eigenvalues numerically, for films with thickness of up to 100 layers without much effort. We discuss some of the results in Sec. IV.

III. STUDIES OF THE CLASSICAL GROUND STATE

In this section, we present a summary of our studies of the classical ground-state spin configuration, for various film thickness and conditions. We have assumed the following about the film geometry, in the calculations reported here: (i) if the film thickness is four layers or less, we have taken the film to be of fcc character, with lattice constant appropriate to bulk Cu, and (ii) for films thicker than four layers, we use a bcc configuration with lattice constant equal to that of bulk Fe. The surfaces are (100) surfaces. The strength of the nearest-neighbor exchange J is adjusted to reproduce, in the long-wavelength limit, the spin-wave exchange stiffness of bulk bcc Fe, which we take to be 2.5×10^{-9} Oe cm^2. The magnetic moment on each site generates a value for $4\pi M_s$ equal to 18 kG, again appropriate for bulk bcc Fe. The quartic contribution to the surface anisotropy [the term proportional to $h_{s_2}(l_\perp)$ in Eq. (1a)] is set to zero for all the calculations reported here.

In the absence of an external field, if h_{s_1} for the monolayer is chosen large enough for the magnetization of the monolayer to be perpendicular to the film (this occurs when h_{s_1} exceeds 9 kG), then as additional layers are added, one reaches a critical thickness where the addition of one layer causes the spins to flop parallel to the surfaces. This is the case where the critical thickness is a few monolayers. For all film thicknesses, and no external field, all spins were either strictly parallel or strictly perpendicular to the surface. For a film just below the critical thickness, addition of one layer "flopped" the spins to the parallel configuration; the angle between the magnetization and the film normal was 90° in the minimum-energy configuration, to all significant figures (four) in the calculation.

In Fig. 2, for ultrathin films with a surface anisotropy

field of 31 kG in each surface, we summarize the equilibrium spin configuration as a function of number of layers, for the case where an external magnetic field is applied parallel to the film surfaces. For these films, the exchange interactions are sufficiently strong that the spins in the various layers are very closely parallel. Thus we show here only the average canting angle. With zero external magnetic field applied, the critical thickness is between three and four layers. That is, the three-monolayer film has all spins strictly normal to the surfaces, and the four-monolayer film has spins strictly parallel to them. Application of a modest magnetic field parallel to the film surfaces induces substantial canting, as illustrated. A field of only 6 kG moves the critical thickness down to the point where in the three-layer film, all spins are strictly parallel to the surfaces.

We have also explored the nature of the classical ground state for films of fixed thickness, as the strength of the easy axis surface anisotropy is increased from zero, where the ground state has spins parallel to the film surfaces. There is a critical value of h_{s_1} for each film thickness, above which canting sets in. As the thickness increases, the critical field increases also.
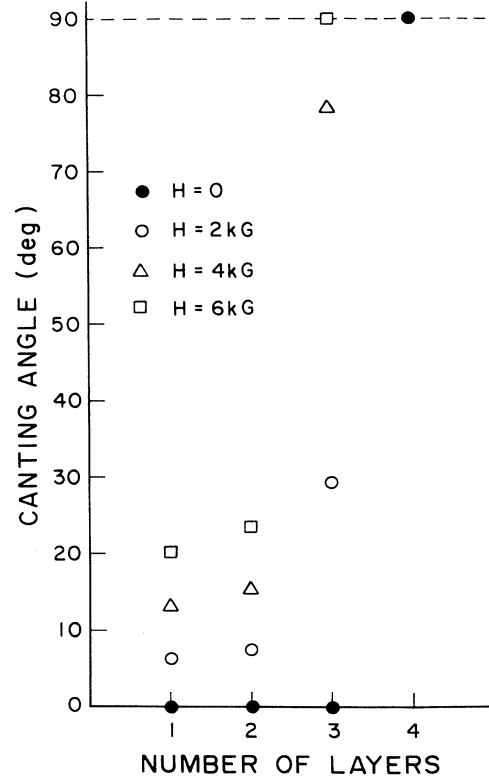
FIG. 2. The canting angle (measured from the film normal) in ultrathin films, with a surface (or interface) anisotropy field $h_{s_1} = 31$ kG acting in each outer surface. We show the canting angle for various external fields applied parallel to the surfaces. For all the four-layer films, the canting angle is strictly 90°.

Before we present our results, we recall the results of an analytical description of surface anisotropy induced spin canting, for the semi-infinite ferromagnet.[18] In present notation,[19] for semi-infinite Fe with bulk lattice constant a_0, the critical value of h_{s_1} is given by

$$h_{s_1}^c = 4\pi M_s(1+\xi) \qquad (24)$$

where $\xi = (D/\pi M_s a_0^2)^{1/2}$. For bulk Fe, we have $\xi \approx 26$, so $h_{s_1}^c \approx 486$ kG, a value considerably larger than the surface anisotropies reported for various Fe ultrathin films. It is possible to extend the treatment of Ref. 14 to apply to a film with N layers, separated by the distance $a_0/2$. If we assume each outer layer is subjected to easy axis anisotropy of the identical strength, and treat the film as a continous rather than a discrete set of layers, we find Eq. (24) is replaced by

$$h_{s_1}^c = 4\pi M_s\left[\xi\tanh\frac{N}{2\xi}+1\right]. \qquad (25)$$

In Fig. 3, for a 100-layer bcc film, we show the canting angle as a function of layer number, when the film is subjected to easy axis anisotropy (applied equally to both surfaces) of various strengths. From the numerical work, we find the critical field to be 452 kG; the expression in Eq. (25) gives 467 kG, which is quite close. Right at the critical field, the spins are all arranged parallel to the surfaces. Canting is induced near the surfaces when the critical field is exceeded; the spins twist so that, in the film center, they are more nearly parallel to the surfaces. If the surface anisotropy field exceeds the critical field by only a rather small amount, the canting can be very appreciable in the surfaces. For surface anisotropy fields of 500 kG, just 10% above the critical field, the canting angle in the surfaces is 36°.

In Fig. 4, we plot the critical surface anisotropy field required to induce spin canting, as a function of film thickness. It is assumed the anisotropy is applied equally to both surfaces. The solid line is the prediction of Eq. (25), which accounts for trends rather nicely, though $h_{s_1}^c$ is overestimated a bit. The discrepancy is greatest, as expected, for the thinner films. For five layers, Eq. (25) gives 62 kG as the critical value of h_{s_1}, while the microscopic calculation gives 41 kG, which is substantially smaller. For one through four layers (these are fcc films as mentioned earlier), the numerical work gives 9, 14, 23, and 32 kG, respectively, while Eq. (25) gives, beginning with $N=2$, the values 29, 35, and 40 kG. Thus, for the few-layer films, the microscopic treatment appears to be required for accurate results.

We next turn our attention to the spin-wave excitations of the films such as those explored in the present section.

FIG. 3. A plot of the canting angle as a function of layer number, for a 100-layer bcc film subject to surface anisotropy of easy axis character, of various strengths. The anisotropy is applied equally to both surface layers. The external field is zero.
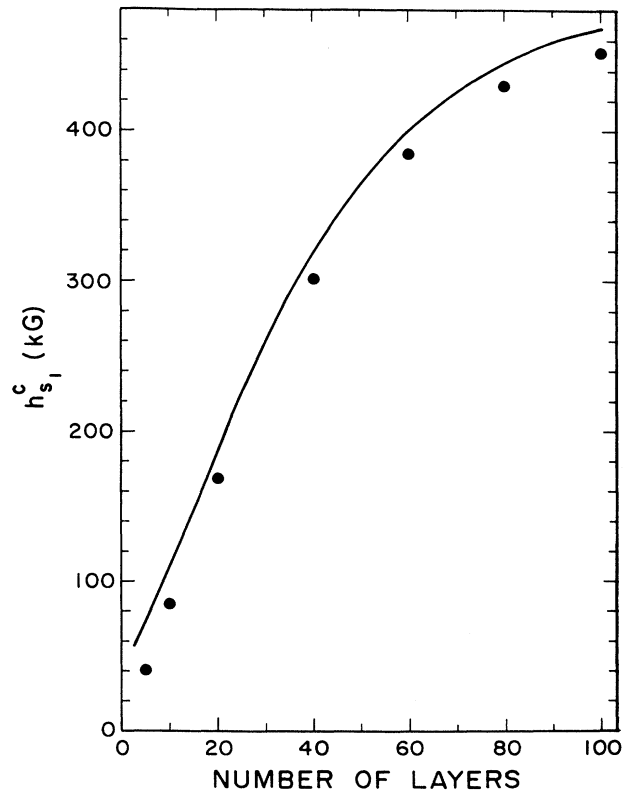
FIG. 4. Numerical calculations of the critical surface anisotropy field to induce spin canting, as a function of film thickness (dots). It is assumed that the anisotropy is applied to both surfaces equally. The solid line is a plot of the prediction of Eq. (25).

IV. MICROSCOPIC STUDIES OF SPIN WAVES IN VERY THIN FILMS

In this section, we present a summary of our studies of spin waves in very thin films, addressing some questions raised earlier. We saw in Sec. III that in the ultrathin film with easy axis anisotropy and no external field applied, the classical ground state is one with spins either normal to the film surfaces, or parallel to them. Application of an external magnetic field parallel to the film surfaces induces spin canting, and ultimately pulls the magnetization over, until it becomes parallel to these surfaces. In a very elegant experiment, Dutcher et al. explored the variation with external field of the lowest-lying spin-wave mode, for a three-monolayer Fe film on Cu(100).[6] Brillouin scattering was used to measure the field dependence of the spin-wave frequency of this study. As the magnetic field approaches the critical value, where the spins just become parallel to the film surfaces, they find the frequency of the mode vanishes, to increase roughly linear with field at higher fields.

In Fig. 5, for our model of a three-layer Fe film, we show our calculation of the field dependence of the low-lying mode. The dots are the data points of Ref. 6. The theoretical curve, calculated for the parameters indicated in the figure caption, bears a close resemblance to the theoretical curve in ref. 6, calculated from macroscopic theory. The authors of Ref. 6 argue that the presence of the quartic terms in $S_\perp(l)$ in Eq. (1a), in addition to the
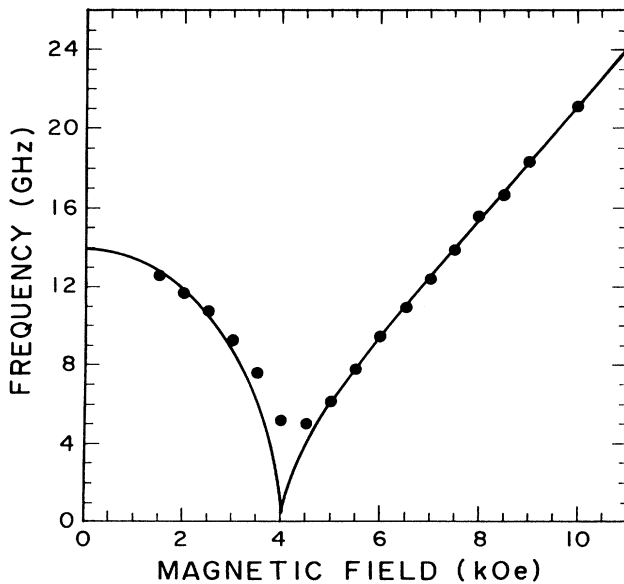
FIG. 5. The magnetic-field dependence of the $k_{||}=0$, low-frequency spin-wave mode of our model of a three-layer Fe film. We assume the parameters h_{s_1} and h_{s_2} of Eq. (1d) have the values 30.9 and 1.68 kG, respectively. We chose $4\pi M_s = 18$ kG, and the exchange constant D such that $D/a_0^2 = 1918$ kG, with $a_0 = 3.6 \times 10^{-8}$ cm. The Landé g factor is 1.95, following Ref. 6. The dots are the data points of Ref. 6.

quadratic terms proportional to h_{s_1}, are required to obtain both the zero field frequency and the critical field at which the mode goes "soft." We agree, and the ratio of h_{s_2} to h_{s_1} we require is very similar to that used by these earlier authors.

Some ultrathin ferromagnetic films have anisotropy of easy plane rather than easy axis character. That is, the direction normal to the plane is a "hard axis," and the magnetization thus lies within the plane of the film. In such a configuration, application of a magnetic field normal to the film will drive the lowest spin-wave mode "soft" at the critical field that tilts the magnetization out of the plane. We know of no such study of soft spin waves in ultrathin films of this nature, but in a very interesting experiment, Demokritov and co-workers have explored this phenomenon in bulk crystals that are quasi-two-dimensional easy plane ferromagnets.[20]

To set the scale for the spin-wave frequencies in Fig. 5, we recall that the three-layer film has three normal modes at $k_{||}=0$; the remaining two are of "optical" character, with frequencies influenced by interplanar exchange couplings. For our model, these frequencies are 7.68×10^3 kG (2.10×10^4 GHz) and 23.0×10^3 kG (6.28×10^4 GHz), respectively. They thus lie very far above the low-lying mode whose frequency is displayed in Fig. 5. This means that to a very excellent approximation, the three-layer film is a quasi-two-dimensional system at room temperature and below, in the sense that the two high-lying branches have excitation energies so large, they will have little influence on the thermodynamic properties of the film. The description we provide here of the field variation of the canting angle gives us a mean-field description of a second-order phase transition, and its associated soft mode. Since, as just remarked, the system is in fact quasi-two-dimensional, the physics of this transition may be richer than this picture implies. We hope to look into this question further.

In Fig. 6, we show the dispersion relation of the lowest spin-wave branch, as a function of the wave vector $k_{||}$, for the three-layer film modeled in Fig. 5. The propagation direction is parallel to the externally applied magnetic field. For the range of wave vectors illustrated, the dispersion relation has a quadratic dependence on wave vector, with curvature influenced only modestly by the external field. The anomalous nature of the dip in frequency calculated for the external field of 4 kOe is an artifact with origin in round-off error, so far as we can tell, owing to the difficulty in determining, to high accuracy, the classical ground state near the critical point of phase transition. While Fig. 6 shows the dispersion for only one direction of propagation, to very high accuracy we find the dispersion curves isotropic.

The behavior in Fig. 6 is very different from that realized in films with macroscopic thickness. In bulk ferromagnets, with Zeeman, dipolar, and exchange couplings included, the limiting frequency of a spin wave depends on the angle between the wave vector and the magnetization, as the wave vector approaches zero. This is true also for the initial curvature in the dispersion relation. For the Damon-Eshbach surface spin waves in
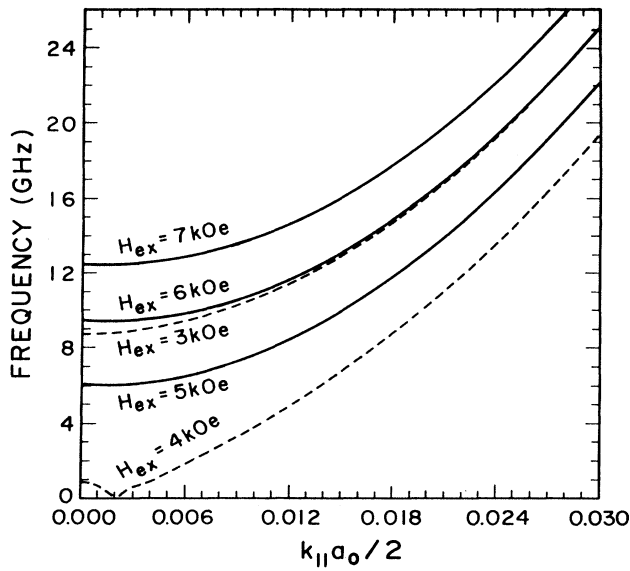
FIG. 6. The dispersion relation of the low-lying spin-wave branch of the three-layer film, for the case where the propagation direction is parallel to the external field. The curves are labeled with the value of the external field. It is assumed the film has fcc structure, and we use the parameters employed in Fig. 5.

macroscopic films, similar statements apply. The frequencies we calculate for the low-lying branch are quite isotropic, as just remarked, even in the domain of frequencies where dipolar and exchange contributions are comparable. We presume the origin of this behavior is that for such thin films, the effective dipolar fields generated by the spin motion are quite uniform over the film.

We now turn to an issue raised in Sec. I, which is the evolution in the character of the surface spin waves with decreasing wave vector, as one makes the transition from the exchange-dominated regime, at large wave vector, to the case of small wave vectors where the excitation energy is dominated by the Zeeman and dipolar contributions. For this purpose, we shall study spin waves in a model film with 100 layers and a bcc structure. We have artifically reduced the strength of the exchange by a factor of 20, causing the exchange modes to drop in frequency; this allows us to explore the interaction between the surface waves and standing spin waves. Surface anisotropy will be set to zero, so all spins lie in the plane parallel to the surfaces. An external field of 1 kG is applied parallel to the [100] direction, that of $\hat{n}_1$ in Fig. 1. We shall confine our attention to propagation for which $k_\parallel$ is perpendicular to the magnetization, that of $\hat{n}_2$ in Fig. 1.

In Fig. 7, for wave vectors $k_\parallel = k_\parallel \hat{n}_2$, which range in magnitude from zero to the surface Brillouin-zone boundary value of π/a_0, we show the dispersion relations of the six lowest-lying spin-wave modes of the film. The scale in the figure is such that at all wave vectors shown, save the regime very close to $k_\parallel = 0$ where detail is not resolved, the exchange energy is the dominant contribution to the
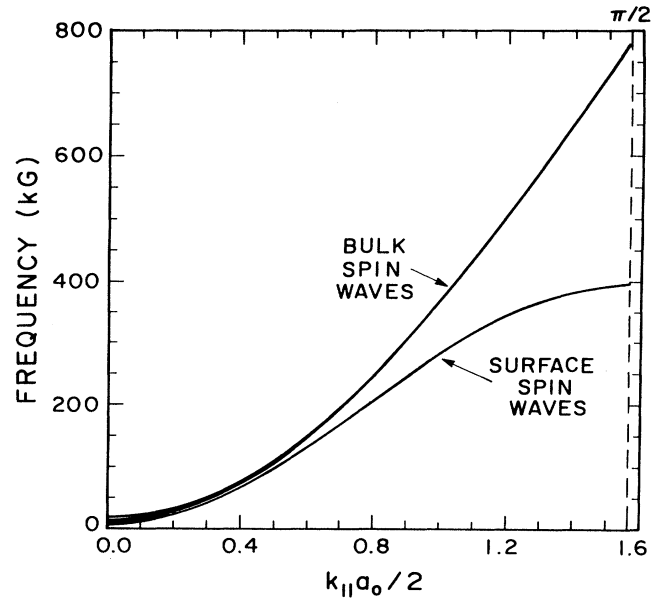
FIG. 7. The first six lowest-lying spin-wave branches for a 100-layer bcc film, with no surface anisotropy. We have decreased the strength of the exchange from that relevant to Fe films by a factor of 20. The lowest-lying curve describes the two nearly degenerate exchange-dominated surface spin waves, and we then show the four lowest-lying standing spin-wave resonances of the film. An external field of 1 kG is applied parallel to the [100] direction.
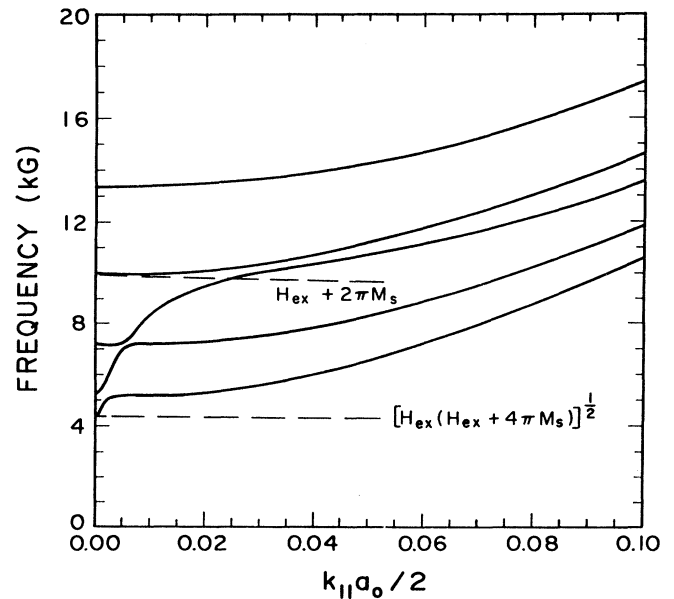
FIG. 8. The lowest six spin-wave branches for the film explored in Fig. 7, for wave vectors near the center of the surface Brillouin zone.

excitation energy. The lowest-lying branch describes the exchange-dominated surface waves; there is one mode localized on each surface, so this is a twofold degenerate branch. Strictly speaking, one should speak of an even and odd parity branch, but for the range of wave vectors emphasized in the figure, the overlap between eigenfunctions localized on the two surfaces is very small. We have the four lowest-lying bulk waves illustrated in the figure also. These dispersion relations agree well with analytic expressions derived for a model which ignores the influence of dipolar couplings.

Before we turn to an examination of the behavior of the waves for small $\mathbf{k}_\parallel$, we recall the description provided by the macroscopic theory of long-wavelength spin waves, within which the role of exchange is ignored. In the bulk, for any wave vector that lies in the plane perpendicular to the magnetization, the spin-wave frequency is independent of wave vector and, in magnetic-field units, equals $[H_{ex}(H_{ex}+4\pi M_s)]^{1/2}$. For a film of thickness d, for each choice of $\mathbf{k}_\parallel$, we have a *single* surface spin wave (not two as in Fig. 7), whose frequency $\Omega_s(\mathbf{k}_\parallel)$ is[9]

$$\Omega_s(\mathbf{k}_\parallel)=[(H_{ex}+2\pi M_s)^2-4\pi^2M_s^2e^{-2k_\parallel d}]^{1/2} . \quad (26)$$

This wave is often referred to as the Damon-Eshbach wave. In the thick film limit $k_\parallel d\gg1$, we thus have $\Omega_s(\mathbf{k}_\parallel)=H_{ex}+2\pi M_s$; here the eigenvector of the surface wave is localized near one of the two film surfaces. As $\mathbf{k}_\parallel\rightarrow0$, the frequency $\Omega_s(\mathbf{k}_\parallel)$ drops to the long-wavelength bulk spin-wave frequency $[H_{ex}(H_{ex}+4\pi M_s)]^{1/2}$. For all values of $\mathbf{k}_\parallel$, the surface wave frequency $\Omega_s(\mathbf{k}_\parallel)$ lies *above* the long-wavelength bulk frequency.

It is interesting to inquire, as remarked in Sec. I, how the transition between these two regimes occurs.

In Fig. 8, we show the behavior of the lowest six branches of the film explored in Fig. 7 for wave vectors near the center of the surface Brillouin zone. At the smallest wave vectors, we see the trajectory of a mode that follows Eq. (26), beginning at $\mathbf{k}_\parallel=0$ at the frequency $[H_{ex}(H_{ex}+4\pi M_s)]^{1/2}$, and initially rising linearly with
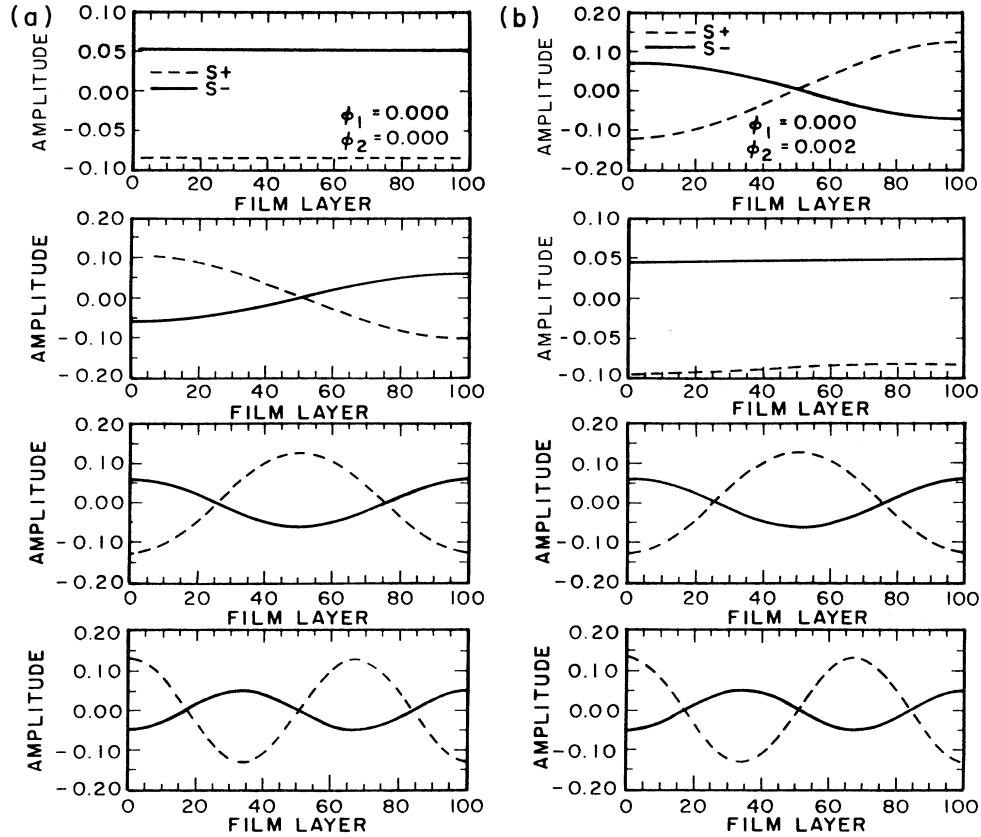
FIG. 9. The eigenvectors of the four lowest-lying modes of the 100-layer bcc film discussed in Sec. IV. The dashed lines are plots of the amplitude corresponding to S_+ and the solid lines are for S_-. We have $\phi_1=k_1a_0/2$ and $\phi_2=k_2a_0/2$. The 1-2 plane coincides with the film surfaces, and the magnetization $\mathbf{M_s}$ lies in the 1 direction. We show eigenvectors for (a) $\phi_1=\phi_2=0.000$ and (b) $\phi_1=0.000$, $\phi_2=0.002$.

$k_{\parallel}$. There are repeated hybridizations with modes whose dispersion curves it crosses. This branch begins to flatten out as if it were to approach the asymptotic frequency $H_{ex}+2\pi M_s$ (see the third branch from the bottom, near $k_{\parallel}a_0/2\approx0.020$), but its frequency is lifted upward past the asymptote by the influence of exchange. At the largest wave vector in the figure, one can see that the two lowest-frequency branches are beginning to converge, to form the pair of surface spin-wave modes displayed in Fig. 7. In essence, as the wave vector increases, the Damon-Eshbach wave of magnetostatic spin-wave theory disappears into the forest of standing spin-wave modes, while the bottom two normal modes slowly evolve into the exchange-dominated surface waves, with increasing wave vector.

It is interesting to examine the variation with wave vector of the eigenvectors associated with the various spin-wave modes just discussed. The eigenvectors are displayed in Fig. (9)–(11) and the direction of propagation is $\mathbf{k}_{\parallel}=k_{\parallel}\hat{\mathbf{n}}_2$, equivalently expressed in terms of phase factors as $\phi_1=0$ and $\phi_2=k_{\parallel}a_0/2$.

In Fig. 9(a), we show the eigenvector at $\phi_1=\phi_2=0$.

The lowest mode is the "uniform mode," with frequency $[H_{ex}(H_{ex}+4\pi M_s)]^{1/2}$. As $\mathbf{k}_{\parallel}\rightarrow0$, the Damon-Eshbach surface mode in fact degenerates into the "uniform mode" of ferromagnetic resonance theory.[21] The next few modes then have the appearance of standing spin-wave modes, in which the "zero slope" boundary condition appropriate to the absence of pinning is utilized.

The "uniform mode," which we recognize as the long-wavelength limit of the Damon-Eshbach wave, has a dispersion relation that is initially linear in wave vector, as suggested in Eq. (26). By the time $\phi_2=0.002$ (with $\phi_1=0$), the lowest branch has crossed the next highest branch, as indicated by the eigenvectors illustrated in Fig. 9(b). In Fig. 10(a), the "uniform mode" is now higher in frequency than the two lowest standing-wave resonances. The quotes have been added to the phrase "uniform mode," because we see some modulation in the profile of the spin-wave eigenvector. With increasing wave vector, this character becomes more pronounced, as we see from the eigenvector with $\phi_2=0.020$. The Damon-Eshbach wave has eigenvector influenced importantly by its mixing with bulk spin waves.
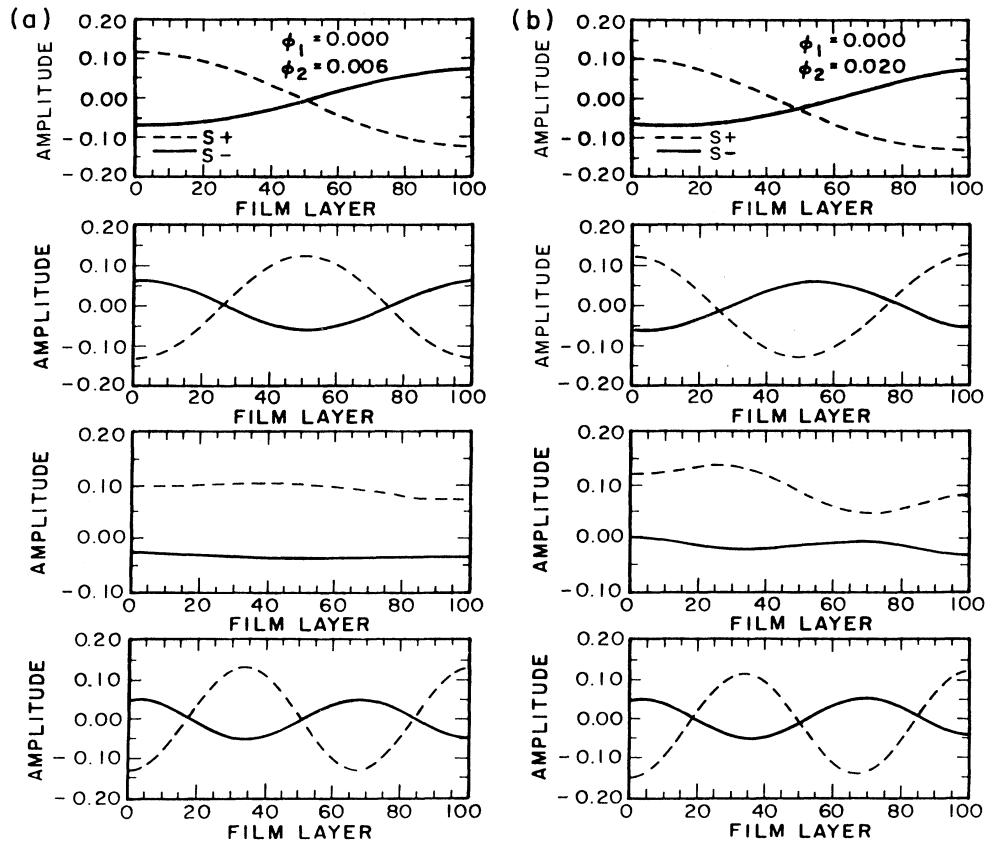
FIG. 10. The same as Fig. 9, except we have eigenvectors for (a) $\phi_1=0.000$, $\phi_2=0.006$ and (b) $\phi_1=0.000$, $\phi_2=0.020$.
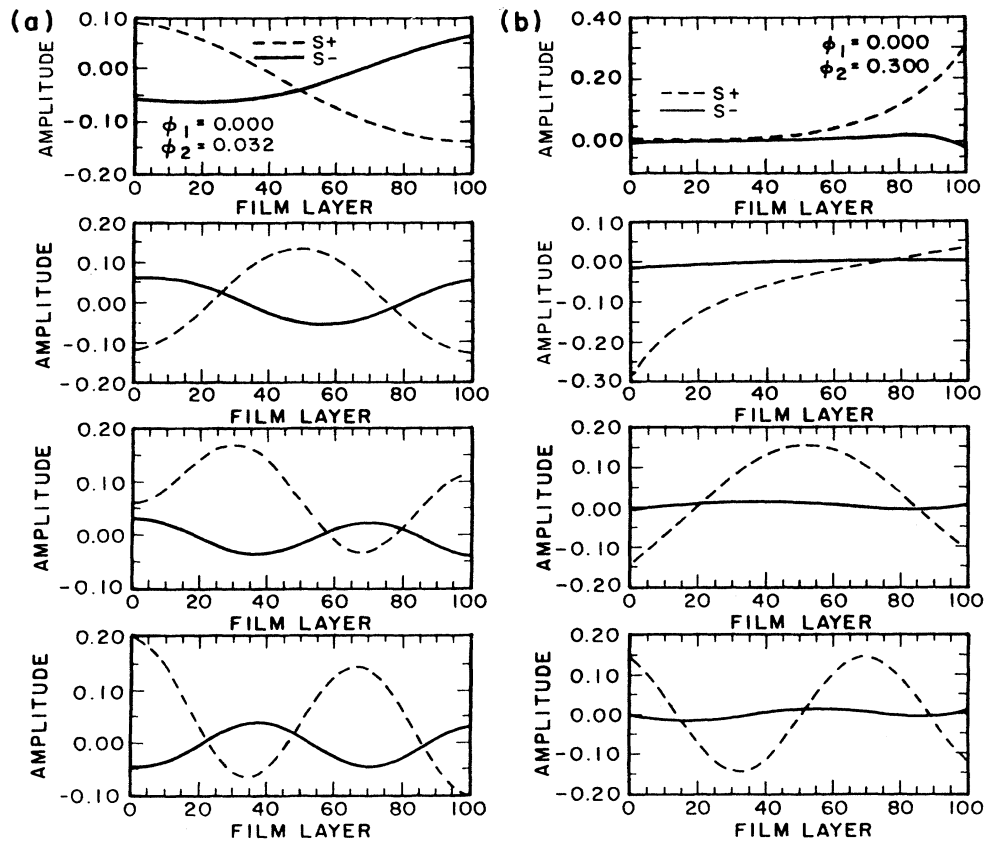
FIG. 11. The same as Fig. 9, except we have eigenvectors for (a) $\phi_1 = 0.000$, $\phi_2 = 0.032$ and (b) $\phi_1 = 0.000$, $\phi_2 = 0.300$.

For $\phi_2 = 0.032$, the low-lying modes all have the character of standing wave resonances; the Damon-Eshbach wave has dissolved into the sea of standing wave resonances. It should be noted that in this regime of wave vector, where both dipole and exchange influence the excitation energy importantly, the modes are not described by eigenvectors with well-defined parity. This is a consequence of the dipole-dipole interactions.

With further increase in wave vector, the two modes of lowest frequency evolve into the surface spin waves of the pure exchange model. We illustrate this in Fig. 11(b). In the pure exchange problem, we should have even and odd parity modes. Examinations of the two highest-frequency modes shows that there remain appreciable quantitative departures from even or odd parity character; this far into the zone, the dipolar interactions still assert themselves. The two lowest modes, the surface waves, show dramatic asymmetries. This could be numerical error. The modes lie very close in frequency, and

in such a case the diagonalization routine may provide a linear combination of the correct eigenvectors for each frequency, believing the modes to be degenerate. The effect may be real; the frequency splitting between the two modes is small, and the eigenvectors of the pure exchange problem may readily be mixed by the residual dipolar interactions, to generate the asymmetric forms shown in Fig. 11(b). We found it difficult to discriminate between these two possibilities in a reliable manner.

It should not prove difficult to use eigenvectors and eigenvalues generated from the present analysis as the basis of studies of the thermodynamic properties of the very thin films examined here. We have initiated such studies, along with extensions to multilayer structures.

ACKNOWLEDGMENTS

[1]B. Heinrich, A. S. Arrot, J. F. Cochran, S. T. Purcell, K. B. Urquhart, and K. Myrtle, J. Cryst. Growth **81**, 562 (1987); B. Heinrich, K. B. Urquhart, A. S. Arrot, J. F. Cochran, K. Myrtle, and S. T. Purcell, Phys. Rev. Lett. **59**, 1756 (1987); J. F. Dutcher, J. F. Cochran, B. Heinrich, and J. S. Arrott, J.

Appl. Phys. **64**, 6095 (1988). Also see N. C. Koon, B. T. Jonker, F. A. Volkening, J. J. Krebs, and G. A. Prinz, Phys. Rev. Lett. **59**, 2463 (1987).

[2]For a qualitative discussion of this point, see Ref. 6 of M. Bander and D. L. Mills, Phys. Rev. B **38**, 12 015 (1988).

[3]D. P. Pappas, K. P. Kamper, and H. Hopster, Phys. Rev. Lett. **64**, 3179 (1990).

[4]B. Heinrich, S. T. Purcell, J. R. Dutcher, K. B. Urquhart, J. F. Cochran, and A. S. Arrott, Phys. Rev. B **38**, 12 879 (1988).

[5]See the chapter by P. Grunberg, in *Light Scattering from Solids V*, edited by M. Cardona (Springer-Verlag, Heidelberg, 1989).

[6]J. R. Dutcher, J. F. Cochran, I. Jacob, and W. F. Egelhoff, Jr., Phys. Rev. B **39**, 10 430 (1989).

[7]J. Sandercock, J. Appl. Phys. **50**, 7784 (1979).

[8]We have such calculations under way at the present time.

[9]D. L. Mills, in *Surface Excitations*, edited by V. M. Agranovich and R. Loudon (Elsevier, Amsterdam, 1984), p. 379.

[10]See, for example, R. E. Camley, T. S. Rahman, and D. L. Mills, Phys. Rev. B **23**, 1226 (1978).

[11]R. E. Camley and D. L. Mills, Phys. Rev. B **18**, 4821 (1978).

[12]H. Benson and D. L. Mills, Phys. Rev. **178**, 839 (1969).

[13]See, for example, C. J. Bradley and A. P. Cracknell, *The Mathematical Theory of Symmetry in Solids* (Clarendon, Oxford, 1972), p. 52.

[14]T. Holstein and H. Primakoff, Phys. Rev. **58**, 1098 (1940).

[15]C. Kittel, *Quantum Theory of Solids*, revised ed. (Wiley, New York, 1987), Chap. 4; J. B. Parkinson, J. Phys. Chem. **2**, 2012 (1969).

[16]R. R. P. Singh, P. A. Fleury, K. Lyons, and P. E. Sulewski, Phys. Rev. Lett. **62**, 2736 (1989).

[17]Talat S. Rahman and D. L. Mills, Phys. Rev. B **20**, 1173 (1979).

[18]D. L. Mills, Phys. Rev. B **39**, 12 306 (1989).

[19]In the present paper, as noted earlier, D is the spin-wave exchange stiffness. The parameter D in Ref. 18 is proportional to the exchange stiffness, but is smaller than it by a factor of 4 for the example considered. Also, our h_{s_1} corresponds to the parameter H_s of Ref. 18.

[20]S. O. Demokritov *et al.*, Zh. Eksp. Teor. Fiz. **95**, 2211 (1989) [Sov. Phys.—JETP **68**, 1277 (1989)].

[21]See C. Kittel, *Introduction to Solid State Physics*, 2nd ed. (Wiley, New York, 1953), p. 410.